J. Mt. Sci. (2011) 8: 728–738
DOI: 10.1007/s11629-011-2038-2

Monitoring and Warning of Landslides and Debris Flows Using an Optical Fiber Sensor Technology

PEI Huafu[1], CUI Peng[2], YIN Jianhua[1]*, ZHU Honghu[3], CHEN Xiaoqing[2], PEI Laizheng[2], XU Dongsheng[1]

1 Department of Civil and Structural Engineering, the Hong Kong Polytechnic University, Hong Kong, China

2 Institute of Mountain Hazards and Environment, CAS, Chengdu 610041, China

3 School of Earth Sciences and Engineering, Nanjing University, Nanjing 210093, China

**Corresponding author, e-mail: cejhyin@polyu.edu.hk*

© Science Press and Institute of Mountain Hazards and Environment, CAS and Springer-Verlag Berlin Heidelberg 2011

Abstract: Landslides and debris flows are typical geo-hazards which occur in hilly or mountainous regions. Debris flows may result from landslides. Geotechnical instrumentation plays an important role in monitoring and warning of landslides and resulted debris flows. Traditional technologies for monitoring landslides and debris flows have certain limitations. The new optical fiber sensors presented in this paper can overcome those limitations. This paper presents two new optical fiber sensor systems: one is the Fiber Bragg Grating (FBG)-based in-place inclinometer for monitoring landslides and the other is the FBG-based column-net system for monitoring debris flows. This paper presents the calibration results of FBG-based in-place inclinometers in laboratory. It is found that the calibration results are in good agreement with theoretical results. Both the FBG-based in-place inclinometers and the FBG-based column-net system have been installed at a site in Weijiagou valley, Beichuan County, Sichuan Province of China. Some preliminary results have been obtained and reported in the paper. The advantages of the FBG monitoring systems and their potential applications are also presented.

Keywords: Landslide; Debris flow; Fiber Bragg Grating; In-place inclinometer; Column-net system

Received: 18 August 2010
Accepted: 9 June 2011

Introduction

Weijiagou is located at Renjiaping Village, Beichuan County (30.40° N, 103.47° E), Sichuan Province of China. Landslides and debris flows occurred frequently in Weijiagou after the Wenchuan earthquake on 12th May 2008 (Cui et al. 2011; Tang et al. 2009; Zhuang et al. 2010). In the earthquake zones, the geo-materials in the top layers of the most mountainous areas are extremely loose due to the heavy earthquake. These loose geo-materials may result in tremendous geological hazards when rainwater infiltrates into the soil mass or rushes with soil and block after heavy rainfall. For instance, a heavy rainfall of 173.8 mm occurred on 23rd September 2008 in Beichuan County, and an additional rainfall of 57.9 mm occurred in the next morning. These heavy rainfalls triggered extensive landslides and debris flows in Weijiagou Valley, the upper area of Beichuan County (Figure 1). The debris flows ran all the way along Weijiagou Valley to the central earthquake-affected Beichuan County. A large part of Beichuan County was buried by the debris flows (Figure 2). In the hills next to Weijiagou, a number of buildings that survived from the earthquake were

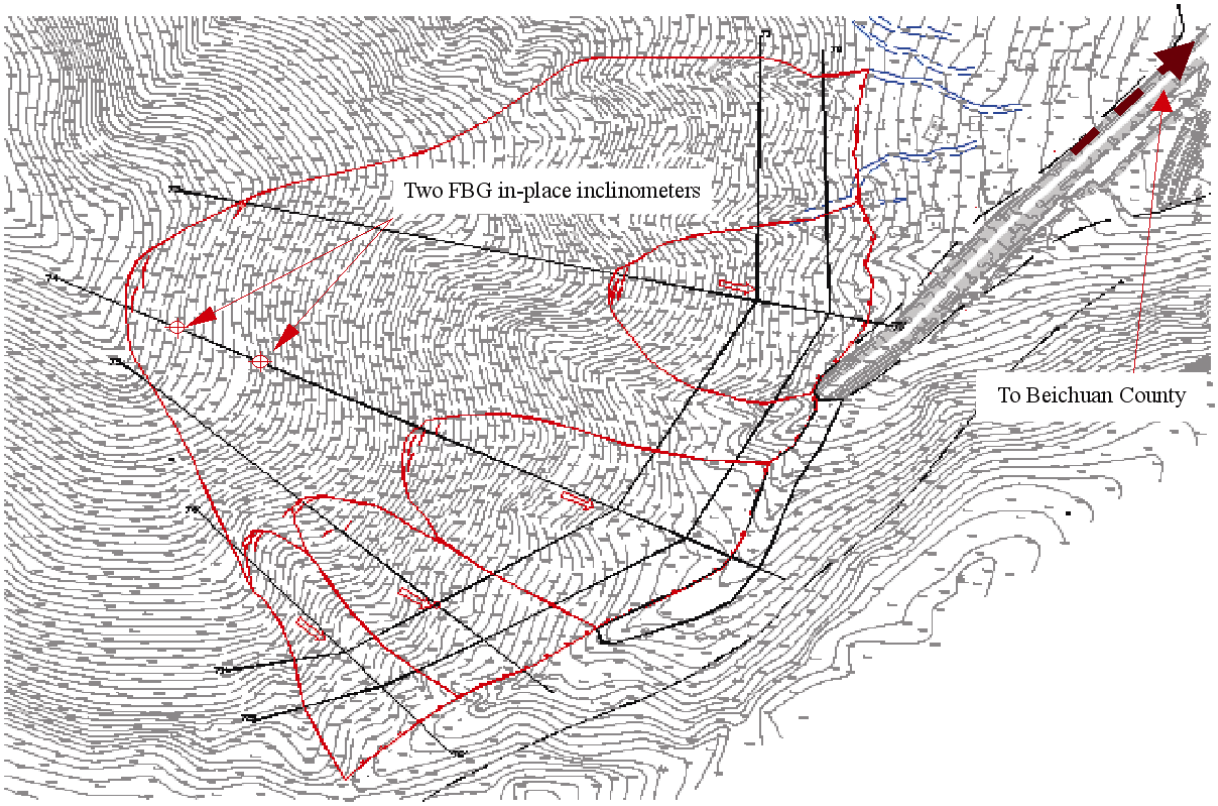

Figure 1 Topographic map of Weijiagou where landslides and debris flows occurred

severely damaged, which results in 22 fatalities (Cui et al. 2009).

Thus, the monitoring and warning on landslides and debris flows are very urgent in order to avoid loss of property and human life. The inclinometer has already been certified to be one of the most effective and reliable instruments nowadays, and has been widely utilized for internal displacements measurement of slopes or other geotechnical structures. Traditional inclinometer systems are classified into two types, including portable inclinometer systems and in-place inclinometer systems. The portable inclinometer system consists of a data collection device and an electric-based probe for inclination detection. This inclinometer is very popular for engineers but it needs two engineers to manipulate this system and pull the cables of probe inside the pre-installed inclinometer casing in a borehole. One in-place inclinometer system can be instrumented for one borehole, but it saves a lot of labor and also can be used for real time field monitoring. In-place inclinometer systems are widely used for monitoring internal displacements of slopes and other geotechnical structures (Dunnicliff 1993). However, these inclinometers have disadvantages, for instance, (a) a large number of cables are required for one borehole; (b) there is an electromagnetic interference problem; (c) signal loss in long distance transmission; and (d) the long-term reliability is low. For debris flows monitoring, geophones are usually used. However, this technology suffers from certain limitations: (a) they also have an electromagnetic interference

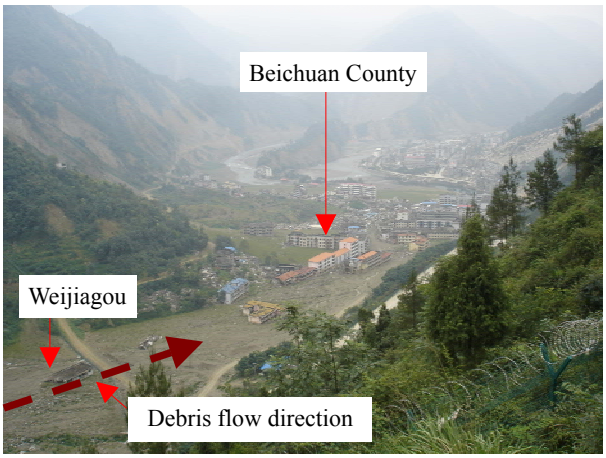

Figure 2 A large part of Beichuan County was buried by the debris flows

problem; (b) noises and vibrations affect the detection of debris flows; (c) if the debris flow happens far away from the monitoring station, the signal may be too weak to be detected.

Hill et al. (1978) firstly fabricated a Fiber Bragg Grating (FBG). Since then, FBG sensing technology has been proposed and utilized for structural health monitoring. Many kinds of FBG-based sensors have been developed such as strain gauges, temperature sensors, pressure sensors, displacement sensors and so on.

The FBG sensing technology has also been successfully utilized for slope stability monitoring (Posey et al. 1999; Yoshida et al. 2002). Lin et al. (2007) developed a new debris flow monitoring system by means of fiber optic interferometers. Experimental results indicate that this fiber optic geophone sensing system works well for low frequency range.

In recent years, researches have been conducted to develop new types of inclinometers based on optical fiber sensing (FBG) technique (Moyo et al. 2005; Yin et al. 2008; Zhu et al. 2010). Ho et al. (2006) fabricated a new type of FBG sensing technique, but it depends on the tiltmeter mechanism.

The scholars in University of Cambridge (Hisham et al. 2011) utilized distributed fiber optic strain sensing technique to investigate lateral deformation for piles on site. However, it is quite difficult to constrain the displacement of optical fiber in one certain lateral direction absolutely, and the accuracy of distributed fiber optic strain sensing technique is not as high as FBG sensing technique. The authors (Pei et al. 2010) fabricated smart standard PVC (Polyvinyl chloride) casing embedded with two series of FBG strain and temperature sensors in certain positions. Differential method was used to calculate the displacements distribution in different depths. But it is very difficult to avoid accumulated error in the strain integration and displacement superposition process.

In this paper, the authors present a monitoring system consisting of FBG-based in-place inclinometers and column-nets for monitoring movements of landslides and warning of debris flows. The development, calibration and field installation of these instruments are presented in details. Furthermore, preliminary monitoring results are analyzed, based on which some findings concerning the performance of the Weijiagou landslides and debris flows are mentioned.

1 FBG sensing Technique and Scientific Principle

An FBG is written into a segment of single-mode fiber in which a periodic modulation of the core refractive index is formed by exposure to a spatial pattern of ultraviolet light. The periodic structure can be created either by interference or by using an appropriate phase mask.

According to Bragg's law, when a broadband source of light has been injected into the fiber, FBG reflects a narrow spectral part of light at a certain wavelength, which is dependent on the grating period and the refractive index of fiber (Morey et al. 1989), as shown in Figure 3. The wavelength at which the reflectivity peaks is called the Bragg wavelength and can be calculated by

$$\lambda_B = 2n_{eff}\Lambda \quad (1)$$

where λ_B is the Bragg wavelength, typically 1510 to

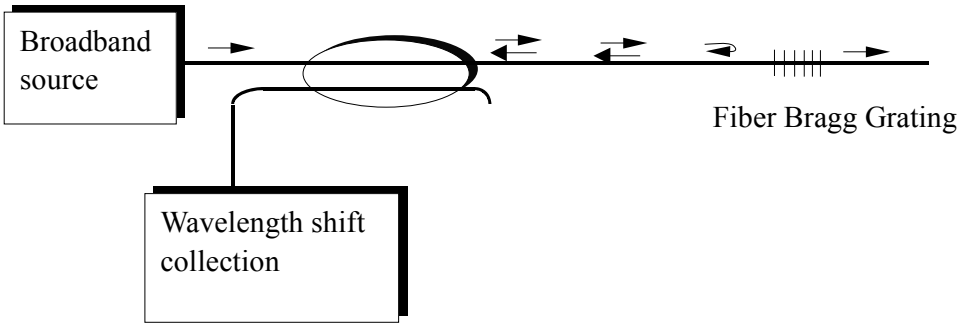

Figure 3 Functioning principle of the FBG sensor

1590 nm; n_{eff} is the effective index of refraction; and Λ is the periodicity of the index modulation.

Considering a standard single-mode silica fiber, the relationship between Bragg wavelength, strain and temperature of the sensing fiber can be simplified as follow (Othonos and Kalli 1999):

$$\frac{\Delta\lambda_B}{\lambda_{B0}} = c_1\varepsilon + c_2\Delta T \tag{2}$$

where c_1 and c_2 are constants, for germanium-doped silica fiber, $c_1 = 0.78$, $c_2 = 6.67\times10^{-6}/{}^oC$; λ_{B0} is the initial Bragg wavelength of the grating under strain-free condition.

2 Development of the FBG in-place Inclinometer

2.1 Working principle

According to classical indeterminate beam theory, the strain distribution on the indeterminate beam is related to the perpendicular force and moment applied on the rigid tip which can be derived from rotation angle and displacement of one rigid tip of the boundary due to material deformation theory. FBG sensors are adhered on the opposite positions of the bar shown as Figure 2. Two pairs of FBG strain sensors are adhered on two cross-sections.

Two measuring points are monitored by FBG strain sensors along the indeterminate beam. The bending strain can be computed by a pair of FBG strain sensors, and wavelength shift due to temperature variation will be compensated by the minus between these two sensors. For a pure bending beam, all strains along it come from the bending moment, but axial extension or shorten deformation will happen. So the pair of FBG strain sensors will delete the strain due to axial strain which avoid the complex stress state effectively.

According to classical indeterminate beam theory (Figure 4), the angle and deflection of the rigid end can be formulated as

$$\tan\theta_B = \frac{L}{R}\frac{L_{FBG1}-L/2}{L_{FBG2}-L_{FBG1}}(\varepsilon_2-\varepsilon_1) - \frac{L}{R}\varepsilon_1 \tag{3}$$

$$v_B = \frac{L^2}{6R}\frac{3L_{FBG1}-L}{L_{FBG2}-L_{FBG1}}(\varepsilon_2-\varepsilon_1) - \frac{L^2}{2R}\varepsilon_1 \tag{4}$$

In the new FBG in-place inclinometer, a smart bar is employed, which is inserted in a

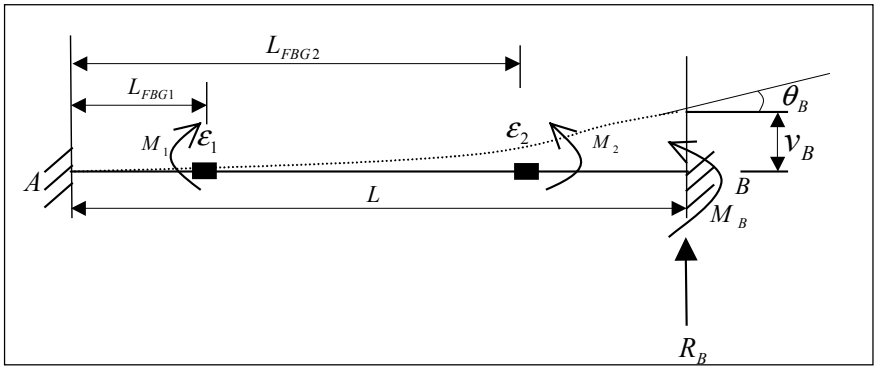

Figure 4 Schematic demonstration of stress state of an indeterminate beam

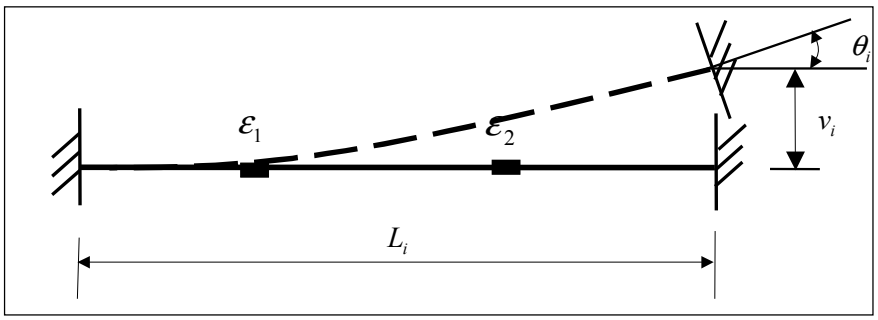

Figure 5 Schematic illustration of an indeterminate beam with two strain sensing points

conventional inclinometer and functions as a beam (Figure 5). A series of FBG sensors were glued on the bar in the longitude direction. The relationships between the strains of the FBG sensors and the displacement and angle of the bar tip can be expressed by

$$v_i = C_1(\varepsilon_2 - \varepsilon_1) - C_2\varepsilon_1 \quad (5)$$

$$\tan\theta_i = C_3(\varepsilon_2 - \varepsilon_1) - C_4\varepsilon_1 \quad (6)$$

where v_i and θ_i are the displacement and the rotation angle of the free end, respectively; C_1, C_2, C_3 and C_4 are four calibration coefficients.

2.2 Laboratory calibration tests

In laboratory calibration tests, displacements and rotational angles are applied on the free end in stages using two translation stages (Figure 6). Linear variable displacement transducers (LVDTs) are used to measure the lateral displacement of the loading points. Strains measured by FBG1 and FBG2 were recorded at the same time.

From the calibration test results (Figure 7), the calibration coefficients C_1, C_2, C_3 and C_4 are calculated to be 0, 38.596, 0 and 100.884, respectively. Displacement and rotation angle of the smart bar under arbitrary loading condition can therefore be obtained using Equations (5) and (6). When a series of sensing bars are connected to each other and inserted into an inclinometer casing (Figure 8), the displacement profile along the inclinometer casing can be calculated section by section in the followings:

For Section 1,

$$d_1 = v_1 + \Delta v_1 = v_1 + \Delta L_1 \sin\theta_1 \quad (7)$$

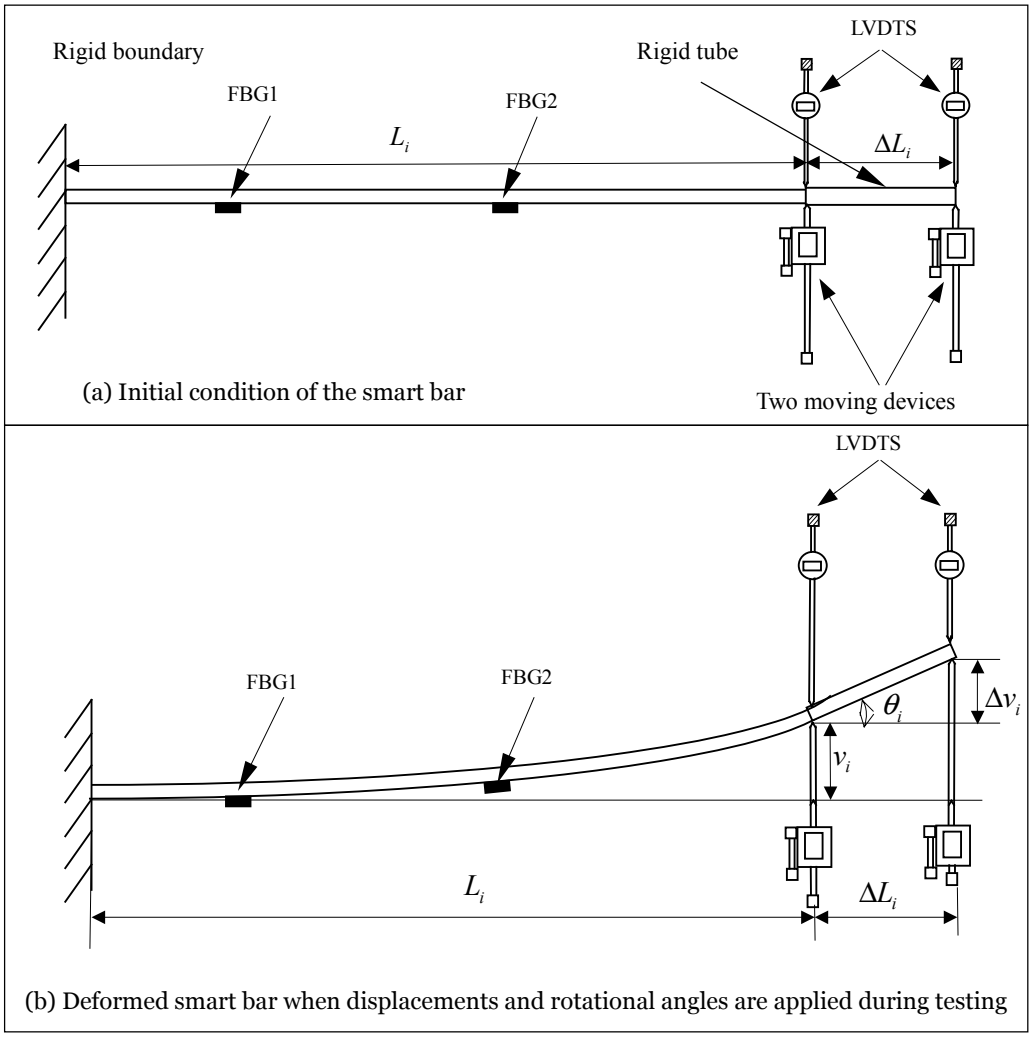

Figure 6 Calibration test setup of the FBG in-place inclinometer

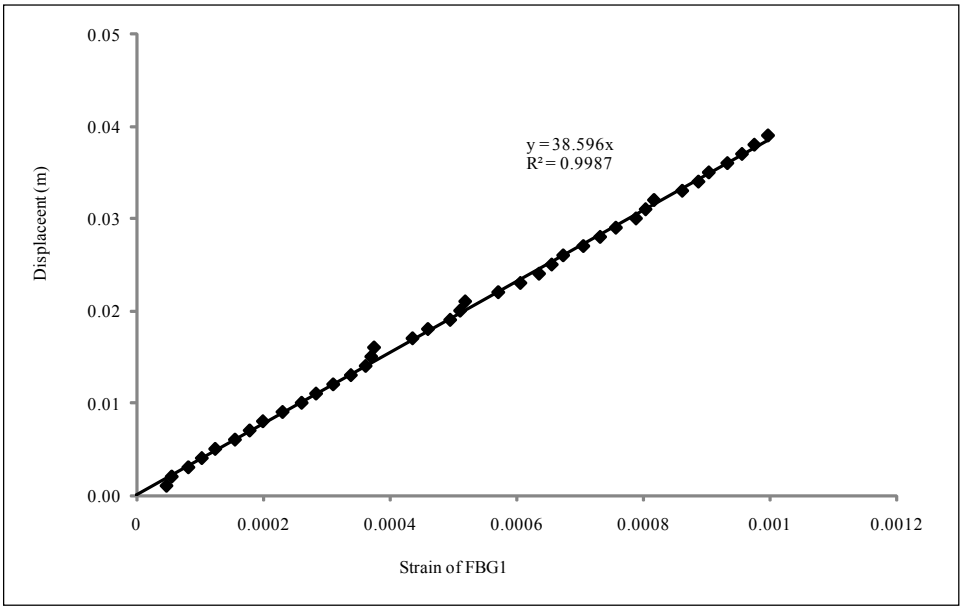

(a) Calibration result for displacement

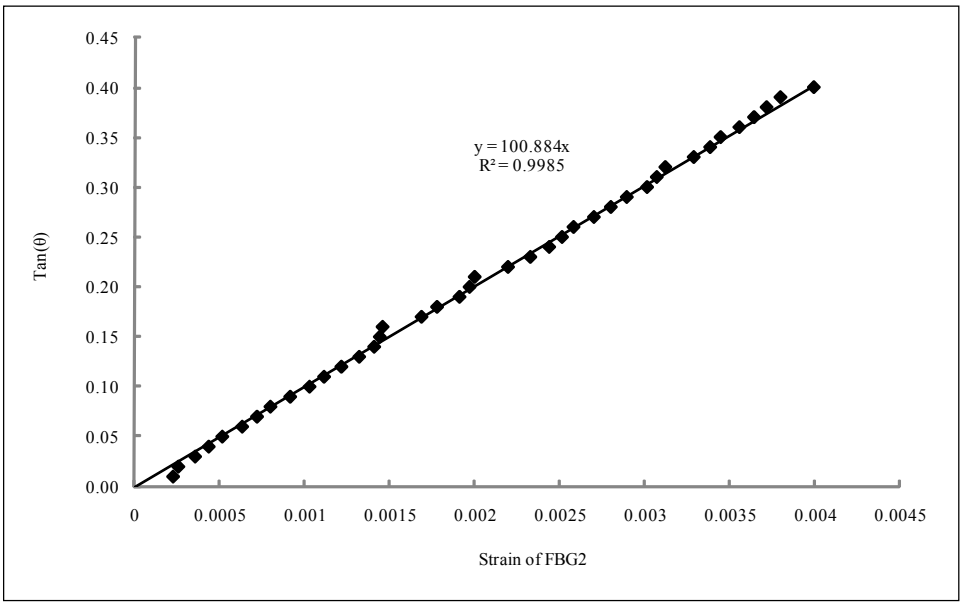

(b) Calibration results for angle

Figure 7 Typical calibration results of the FBG in-place inclinometer

where v_1 is the lateral deflection of the flexible sensor bar; $\Delta v_1 = \Delta L_1 \sin\theta_1$ is the lateral deflection due to rotation (θ_1) of the rigid tube; ΔL_1 is the length of the rigid tube.

For Section 2, the relative lateral displacement is calculated by

$$\Delta d_2 = v_2 + \Delta v_2 = v_2 + \Delta L_2 \sin\theta_2$$

where v_2 is the lateral deflection of the second flexible sensor bar; $\Delta v_2 = \Delta L_2 \sin\theta_2$ is the lateral deflection due to rotation (θ_2) of the second rigid tube; ΔL_2 is the length of the second rigid tube.

Due to the lateral movement and rotation of Section 1, the total lateral movement at the end of Section 2 shall be calculated as:

$$\begin{aligned} d_2 &= d_1 + \Delta d_2 + (L_2 + \Delta L_2)\sin\theta_1 \\ &= v_1 + \Delta L_1 \sin\theta_1 + v_2 + \Delta L_2 \sin\theta_2 + (L_2 + \Delta L_2)\sin\theta_1 \end{aligned} \quad (8)$$

For Section 3, the relative lateral displacement is calculated by

$$\Delta d_3 = v_3 + \Delta v_3 = v_3 + \Delta L_3 \sin\theta_3$$

where v_3 is the lateral deflection of the third flexible sensor bar; $\Delta v_3 = \Delta L_3 \sin\theta_3$ is the lateral deflection due to rotation (θ_3) of the third rigid tube; ΔL_3 is the length of the third rigid tube. Due to the lateral movement and rotation of Sections 1 and 2, the total lateral movement at the end of Section 3 shall be calculated as:

$$\begin{aligned} d_3 &= d_2 + \Delta d_3 + (L_3 + \Delta L_3)\sin(\theta_1 + \theta_2) \\ &= [v_1 + \Delta L_1 \sin\theta_1 + v_2 + \Delta L_2 t \sin\theta_2 + (L_2 + \Delta L_2)\sin\theta_1] \\ &+ (v_3 + \Delta L_3 \sin\theta_3) + (L_3 + \Delta L_3)\sin(\theta_1 + \theta_2) \end{aligned} \quad (9)$$

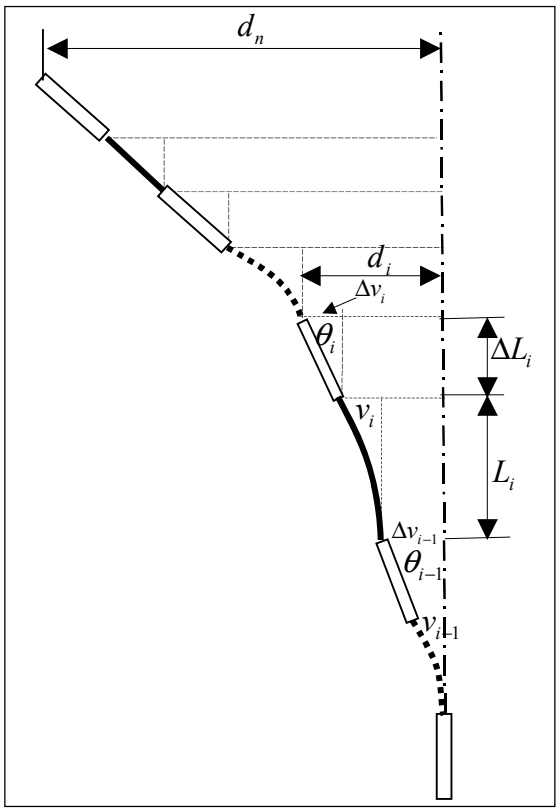

Figure 8 Working principle of FBG in-place inclinometers on site

For Section *i*, the relative lateral displacement is calculated by

$$\Delta d_i = v_i + \Delta v_i = v_i + \Delta L_i \sin\theta_i$$

where v_i is the lateral deflection of the third flexible sensor bar; $\Delta v_i = \Delta L_i \sin\theta_i$ is the lateral deflection due to rotation (θ_i) of the *i*th rigid tube; ΔL_i is the length of the *i*th rigid tube. Due to the lateral movement and rotation of Sections 1 to *i*-1, the total lateral movement at the end of Section i shall be calculated as:

$$\begin{aligned} d_i &= d_{i-1} + \Delta d_i + (L_i + \Delta L_i)\sin(\sum_1^{i-1}\theta_j) \\ &= d_{i-1} + (v_i + \Delta L_i \sin\theta_i) + (L_i + \Delta L_i)\sin(\sum_1^{i-1}\theta_j) \end{aligned} \quad (10)$$

For Section *n*, the relative lateral displacement is calculated by

$$\Delta d_n = v_n + \Delta v_n = v_n + \Delta L_n \sin\theta_n$$

where v_n is the lateral deflection of the *n*th flexible sensor bar; $\Delta v_n = \Delta L_n \sin\theta_n$ is the lateral deflection due to rotation (θ_n) of the *n*th rigid tube; ΔL_n is the length of the *n*th rigid tube. Due to the lateral movement and rotation of Sections 1 to *n*-1, the total lateral movement at the end of Section n shall be calculated as:

$$\begin{aligned} d_n &= d_{n-1} + \Delta d_n + (L_n + \Delta L_n)\sin(\sum_1^{n-1}\theta_j) \\ &= d_{n-1} + (v_n + \Delta L_n \sin\theta_n) + (L_n + \Delta L_n)\sin(\sum_1^{n-1}\theta_j) \end{aligned} \quad (11)$$

3 Development of the FBG Clumn-net System

3.1 FBG column-net system for impact force monitoring

In the newly developed FBG column-net, FBG sensors are glued on the bottom of two steel pipes. A steel wire net is fixed on the pipes that are installed in the debris flow ditch. The FBG sensor can detect the strain at the bottom of the steel pipe where impact forces are applied when debris flow passes by this cross-section.

The drainage area of debris flow (Sichuan Institute of Geological Engineering Investigation 2009) is 1.23 km². The ideal model of the debris flow process in Weijiagou has been proposed by designers (Figure 9).

The relationship between strains of FBG sensors and duration of debris flow can be expressed by

$$\varepsilon_t = \frac{MR}{EI}$$

$$Q_t = \frac{2EI\varepsilon_t}{Rr_c l}$$

$$\varepsilon_t = \frac{\frac{\Delta\lambda_B}{\lambda_{B0}} - c_2\Delta T}{c_1}$$

$$\theta = \frac{Q_t}{t_1} = \frac{2EI\varepsilon_t}{t_1 Rr_c l} \quad (12)$$

The angle θ can be calculated by

$$\frac{Q}{T} = \frac{3}{2}\tan\frac{2EI\varepsilon_t}{t_1 Rr_c l} \quad (13)$$

where R is the outer radius of the steel pipe; Q_t is the current velocity of debris flow; γ_C is the overall density gravity of debris flow; E, I, l are the Young's Modulus, the moment of inertia and the length of the steel pipe column installed on site, respectively; ε_t is the current strain measured by the FBG sensor in debris flow process; and T is the duration of debris flow.

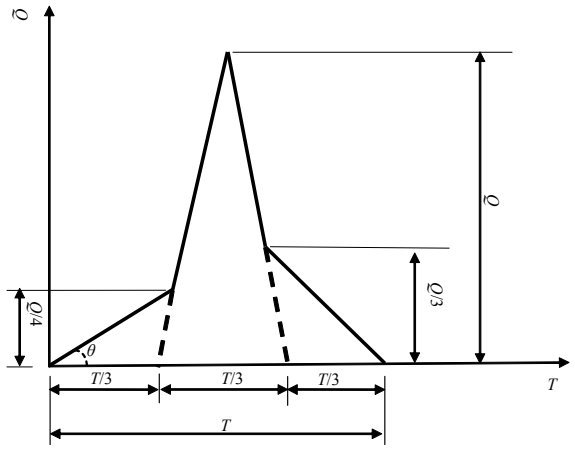

Figure 9 The ideal model of the debris flow process in Weijiagou

The wavelengths of FBG sensors are collected when debris flow blocks on the column-net. The ratio (peak flow volume to duration of single peak debris flow) can be used to evaluate the danger of debris flow. Once the impact force rises up to a certain value, the net will be damaged so that the initiation of primary debris flow process will be detected. Warning of hazardous debris flow can be sent out in advance.

3.2 Laboratory calibration of the FBG column-net system

To conduct laboratory calibration, two FBG sensors were glued on the opposite positions in the same cross section of a steel pipe. The steel pipe is stabilized on the ground (Figure 10). Then uniform loading were applied on the surface of steel column in steps. The test results indicate that there is a linear relationship between the applied force and the Bragg wavelength of the FBG sensor (Figure 11).

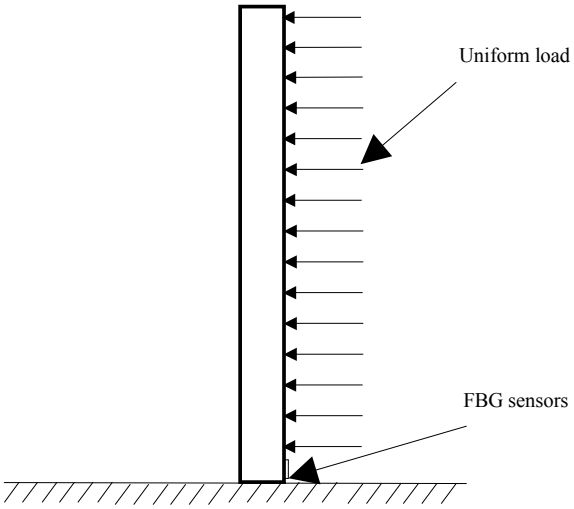

Figure 10 Calibration test of the FBG column-net

4 Implementation of the FBG Sensing and Warning Systems in Weijiagou

4.1 Installation of the FBG system

(1) FBG in-place inclinometers

Two sets of FBG in-place inclinometers are fabricated in laboratory. In every inclinometer, FBG sensors were connected in series using fusion splicer and glued on elastic bars. These bars were connected using steel tubes with sliding wheels which allow the in-place inclinometers to deform with the inclinometer casing installed on site.

The initial wavelengths of all FBG sensors without any deflection were recorded in laboratory. The wavelengths were also recorded after field installation of the inclinometers. The strains of sensors can be calculated by Equation (2), and the displacements and rotation angles of each section

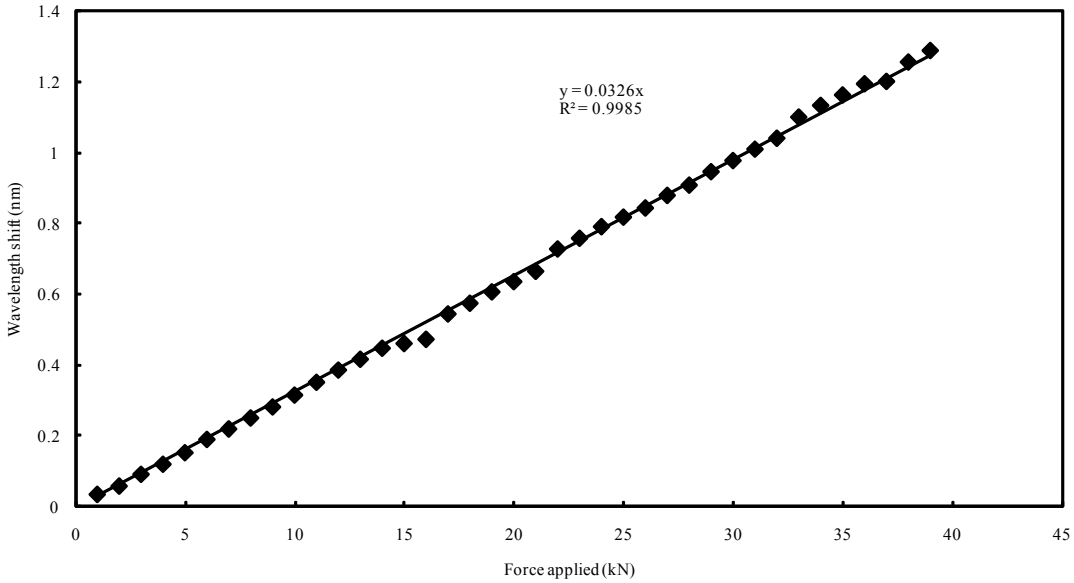

Figure 11 Calibration test of the steel pipe with FBG sensors

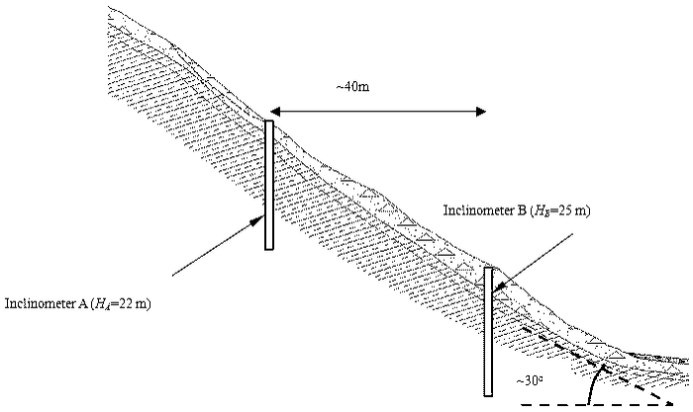

(a) Relative positions of two boreholes with FBG in-place inclinometers in the slope site in Weijiagou

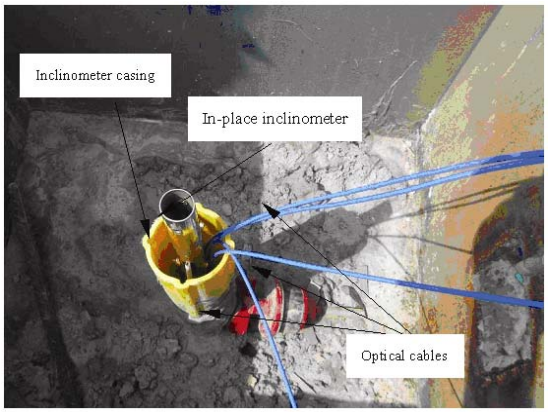

(b) FBG in-place inclinometers installed in an ABS inclinometer casing

Figure 12 Scheme of FBG in-place inclinometers in a borehole on the site in Weijiagou

of the in-place inclinometers can also be computed by Equations (5) and (6).

The inclinometer casings were installed into the slope at the end of 2009 (Figure 12). Since then there were several heavy rainfalls in this site which incur internal stress adjustment and movements of this slope.

(2) FBG column-nets

For Weijiagou debris flow, the diameter of the biggest rock is estimated to be 0.4 m and 1.0 m at the elevation range of 875-650 m and above 875 m, respectively. According to the geological condition of the site under investigation, the maximum

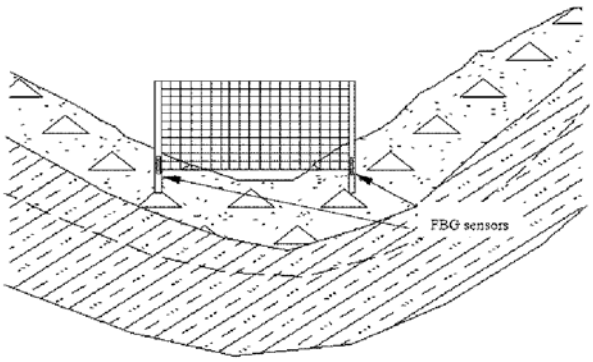

Figure 13 Schematic sketch of an FBG column-net arrangement in one cross-section for monitoring debris flow

diameter of a single block is set to 1 m in this study.

Two steel pipes were grouted into two holes crossing the section of debris flow trench (Figure 13). FBG sensors were glued on to the pipes in the debris flow direction. One metal net was fixed on these pipes. Two FBG column-nets were installed in two cross-sections of the path the debris flow ditch to monitor the mechanism and impact force in the process.

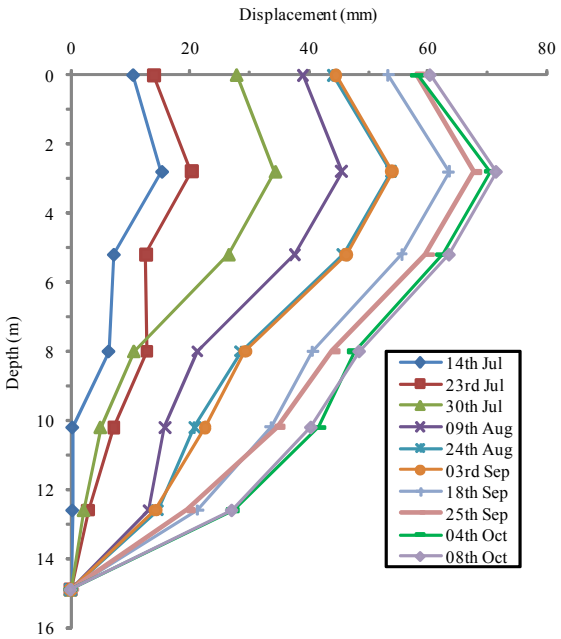

(a) Displacements of Borehole A

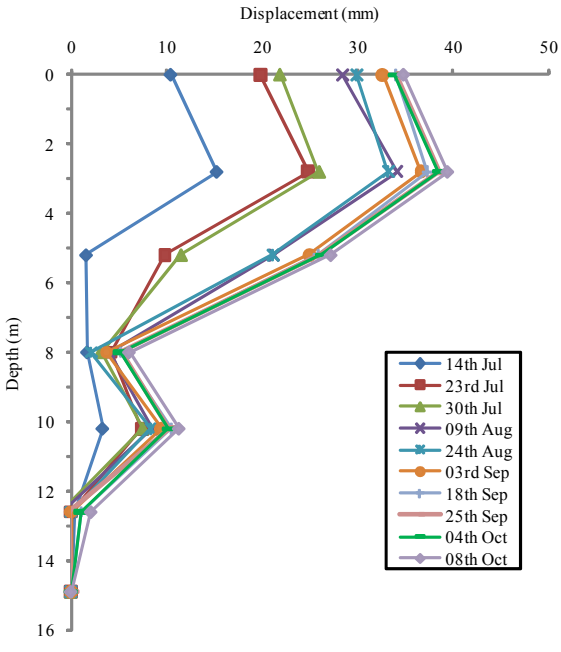

(b) Displacements of Borehole B

Figure 14 Monitoring results from FBG in-place inclinometers in Borehole A and Borehole B at early monitoring stage

4.2 Monitoring results at early stage

Monitoring data were collected on 14th July, 23rd July of 2010 and 30th July of 2010. The displacements and rotational angles of FBG in-place inclinometers in Borehole A and Borehole B at different depths are calculated by Equations (5) and (6). The total displacements of the inclinometer casings are superposed section and section by Equations (7) to (11) (Figure 14). It is found that the movements of geo-materials accumulated gradually and the overall deformation behavior can be defined as shallow sliding. When localized heavy rainfall accumulates to a certain threshold, potential debris flows will be mobilized by shallow landslides.

5 Conclusions

In this paper, a new type of landslide and debris flow monitoring system based on FBG sensing technique is developed and applied in Weijiagou. This system that incorporates the FBG in-place inclinometer and the FBG column-net overcomes certain disadvantages of traditional technologies and satisfies most requirements of landslide and debris flow monitoring, including high accuracy, long-distance transmission and long-term reliability. In order to detect the landslide performance and the mechanism of debris flow during heavy rainfalls, FBG in-place inclinometers and column-nets are installed in Weijiagou. Preliminary monitoring results show that internal movements of the slope are accumulating gradually.

Acknowledgements

The development of the fiber Bragg Grating (FBG)-based in-place inclinometers for monitoring landslides and the FBG-based column-nets for monitoring debris flows is done under the leadership of the co-author Professor YIN Jianhua. The development is supported by research grants

of The Hong Kong Polytechnic University (Grant Nos. G-YE54 and 1-BB7U). The application of the two FBG based monitoring in Weijiaogou is financially supported by the State Key Fundamental Research (973) program project (Grant No. 2008CB425802). In addition, the application of the FBG-based column-net system is supported by a project entitled "Analysis of Geological and Mechanics Reasons Causing Damage of Bridge Structures during Wenchuan Earthquake and Recommendations for Reconstruction" (A/C No. 85G0).

References

Cui P, Chen XQ, Zhu YY, Su FH, Han YS, Liu HJ, Zhuang JQ (2011) The Wenchuan Earthquake (May 12, 2008), Sichuan Province, China, and resulting geohazards. Natural Hazards. 56:19-36.

Cui P, Zhu, YY, Han YS, Chen XQ, Zhuang JQ (2009) The 12 May Wenchuan earthquake-induced landslide lakes: distribution and preliminary risk evaluation. Landslides. 6(3):209-223.

Dunnicliff J (1993) Geotechnical Instrumentation for Monitoring Field Performance. New York, John Wiley & Sons.

Ho YT, Huang, AB, Lee JT (2006) Development of a fibre Bragg grating sensored ground movement monitoring system. Measurement Science and Technology 17(7): 1733-1740.

Hill KO, Fujii F, Johnson DC, Kawasaki BS (1978) Photosensitivity on optical fiber waveguides: application to reflection filter fabrication. Applied Physics Letters 32(10): 647-649.

Hisham M, Kenichi S, Adam P, Peter JB (2011) Performance monitoring of a secant piled wall using distributed fiber optic strain sensing. Journal of Geotechnical and Geoenvironmental Engineering. Doi:10.1061/(ASCE)GT.1943 -5606.0000543.

Lin YL, Lin KH, Chen MH, Lin WW (2007) A debris flow monitoring system by means of fiber optic interferometers. Proceedings of SPIE, Fiber Optic Sensors and Applications V. Boston, USA. pp 6770: 67700Z.1-67700Z.8.

Morey WW, Meltz G, Glenn, WH (1989). Fiber Optic Bragg Grating sensors. Proceedings of SPIE, Boston. 1169: 98-107.

Moyo P, Brownjohn JMW, Suresh R, Tjin SC (2005) Development of fiber Bragg grating sensors for monitoring civil infrastructure. Engineering Structures 27(12): 1828-1834.

Othonos A, Kalli K, Kalli K (1999). Fiber Bragg gratings: fundamentals and applications in telecommunications and sensing. Artech House, Boston.

Pei HF, Yin JH, Zhu HH, Hong CY (2010) In-place displacement monitoring and stability evaluation of slope based on FBG sensing technology. Chinese Journal of Rock Mechanics and Engineering 29(8): 1570-1576. (In Chinese)

Posey RJ, Vohra ST (1999) An eight-channel fiber-optic Bragg grating and stimulated Brillouin sensor system for simultaneous temperature and strain measurements. Photonics Technology Letters 11(12): 1641-1643.

Sichuan Institute of Geological Engineering Investigation (2009) Report on emergency investigation of Beichuan Couty Xishan landslide group (debris flow). (In Chinese)

Tang C, Zhu J, Li WL, Liang JT (2009) Rainfall-triggered debris flows following the Wenchuan earthquake. Bulletin of Engineering Geology and the Environment 68(2): 187-194.

Yin JH, Zhu HH, Fung KW, Jin W, Mak LM, Kuo K (2008) Innovative optical fiber sensors for monitoring displacement of geotechnical structures. The HKIE Geotechnical Division 28th Annual Seminar, Hong Kong: 287-294.

Yoshida Y, Kashiwai Y, Murakami E, Ishida S, Hashiguchi N (2002) Development of the monitoring system for slope deformations with fiber Bragg grating arrays. Proceedings of SPIE, Smart Structures and Materials 2002: Smart Sensor Technology and Measurement Systems. San Diego, USA. pp 296-303.

Zhuang JQ, Cui P, Hu KH, Chen XQ, Ge YG (2010) Characteristics of Earthquake-Triggered Landslides and Post-Earthquake Debris Flows in Beichuan county. Journal of Mountain Science 7(3): 246-254.

Zhu HH, Yin JH, Zhang L, Jin W, Dong JH (2010) Monitoring internal displacements of a model dam using FBG sensing bars. Advances in Structural Engineering 13(2): 249-262.